



HAL
open science

Real-time monitoring of cyclic nucleotide signaling in neurons using genetically encoded FRET probes.

Pierre Vincent, Nicolas Gervasi, Jin Zhang

► **To cite this version:**

Pierre Vincent, Nicolas Gervasi, Jin Zhang. Real-time monitoring of cyclic nucleotide signaling in neurons using genetically encoded FRET probes.. *Brain Cell Biol*, 2008, 36 (1-4), pp.3-17. 10.1007/s11068-008-9035-6 . hal-00342452

HAL Id: hal-00342452

<https://hal.science/hal-00342452>

Submitted on 27 Nov 2008

HAL is a multi-disciplinary open access archive for the deposit and dissemination of scientific research documents, whether they are published or not. The documents may come from teaching and research institutions in France or abroad, or from public or private research centers.

L'archive ouverte pluridisciplinaire **HAL**, est destinée au dépôt et à la diffusion de documents scientifiques de niveau recherche, publiés ou non, émanant des établissements d'enseignement et de recherche français ou étrangers, des laboratoires publics ou privés.

Real-time monitoring of cyclic nucleotide signaling in neurons using genetically-encoded FRET probes

Pierre VINCENT^{1,2}, Nicolas GERVASI^{1,2} and Jin ZHANG³

1: CNRS UMR 7102 Neurobiologie des Processus Adaptatifs, Paris. 9 quai St Bernard, 75005 Paris, FRANCE

2: UPMC UMR7102 Neurobiologie des Processus Adaptatifs, Paris. 9 quai St Bernard, 75005 Paris, FRANCE

3: Department of Pharmacology and Molecular Sciences, Solomon H. Snyder Department of Neuroscience and Department of Oncology, The Johns Hopkins University School of Medicine, Baltimore, Maryland 21205, USA.

pierre.vincent@upmc.fr; jzhang32@jhmi.edu

Abstract: The signaling cascades involving cyclic nucleotides play a key role in signal transduction in virtually all cell types. Elucidation of the spatiotemporal regulation of cyclic nucleotide signaling requires methods for tracking the dynamics of cyclic nucleotides and the activities of their regulators and effectors in the native biological context. Here we review a series of genetically encoded FRET-based probes for real time-monitoring of cyclic nucleotide signaling with a particular focus on their implementation in neurons. Current data indicate that neurons have a very active metabolism in cyclic-nucleotide signaling, which is tightly regulated through a variety of homeostatic regulations.

Cyclic nucleotides; fluorescence imaging

Imaging cyclic nucleotides in neurons

Introduction

A number of neuropsychiatric pathologies are related to impairments of neuromodulatory systems, as demonstrated by the number of drugs used in clinics which target neuromodulators, acting either on reuptake systems or on G-protein coupled receptors. Among the intracellular signaling cascades triggered by neuromodulators, signaling pathways regulated by cyclic adenosine monophosphate (cAMP) and cyclic guanosine monophosphate (cGMP) are known to be responsible for the modulation of many cellular functions in the brain. cAMP, as the prototype second messenger, plays important roles in a wide array

1
2
3
4 of neuronal functions including specific forms of synaptic plasticity, cognitive
5 functions, neuronal survival and axonal regeneration. Many of these responses are
6 mediated by cAMP-dependent protein kinase (PKA), which has served as a model
7 of protein kinase structure and regulation. On the other hand, the exchange protein
8 directly activated by cAMP (Epac) and cAMP-regulated channels are also
9 important cAMP effectors. cGMP is another intracellular second messenger that
10 plays an important signaling role in neurons, particularly in mediating the
11 response to the gas neuromodulator nitric oxide.
12

13
14 Spatial compartmentation of cyclic nucleotide action at the subcellular level was
15 first suggested more than 20 years ago, and recent studies provide new evidence
16 that a general increase in cyclic nucleotide concentration in the cell is not
17 sufficient for the specific regulation of functional effects. For generating
18 appropriate cell responses, precise spatial and temporal control of cyclic
19 nucleotide signaling must be achieved. In order to better understand cyclic
20 nucleotide actions within their signaling context, methods are needed to analyze
21 their dynamics in living cells. Ideally such methods should provide high spatial
22 and temporal resolution for tracking the activity changes continuously and for
23 following them in different compartments and microdomains. Furthermore,
24 quantitative information should be obtained from individual cells, because some
25 important aspects of signal transduction, such as transient and oscillatory activity,
26 can be averaged out during studies of a population of cells. Care must also be
27 taken to ensure that the signal is specific, and that expression of the probe does
28 not perturb the phenomenon that the probe is supposed to report. A major
29 breakthrough in the study of cyclic-nucleotide mediated intracellular signaling has
30 arisen with the new optical biosensors that have been developed since 2001.
31 Genetically encoded probes used to monitor the cAMP/PKA cascade have been
32 reviewed recently (Willoughby and Cooper, 2008; Lohse et al., 2008) and we
33 focus here on applications of FRET-based biosensors that are capable of tracking
34 cyclic nucleotide signaling in living cells with a particular focus on their
35 implementation in neurons.
36
37
38
39
40
41
42
43
44
45
46
47
48
49
50
51
52
53
54
55

56 **Cyclic AMP and PKA**

57
58
59 The first probe constructed to report changes in cAMP concentration was
60 FICRhR (Adams et al., 1991). This probe used chemically labeled PKA subunits
61
62
63
64
65

1
2
3
4 whose dissociation was monitored by FRET. The FICRhR probe was used on
5 some favorable preparations like large invertebrate neurons (Bacsikai et al., 1993;
6 Hempel et al., 1996) or *Xenopus* embryonic neurons (Gorbunova and Spitzer,
7 2002); however, its use in mature vertebrate neurons was limited by the difficult
8 task of introducing the probe as an intact holoenzyme into the cytosol (Vincent
9 and Bruscianno, 2001). Various gene transfer methods now allow the expression of
10 genetically-encoded probes in virtually any cell type including neurons, and
11 probes using CFP and YFP as fluorophores were soon derived from the previous
12 FICRhR (Zaccolo et al., 2000; Lissandron et al., 2005). This assay depends on the
13 coexpression of two genes coding for the two moieties of the probe at a similar
14 level, a condition that must be achieved for proper functioning of the probe.
15 Unfortunately, these PKA-derived probes have an intact kinase domain, so the
16 presence of the probe inherently increases PKA activity inside the cell. This has
17 been reported with FICRhR in cardiomyocytes where probe diffusion into the cell
18 partially activated L-type calcium channels (Goaillard et al., 2001). Neurons have
19 a tonic cAMP production and PKA activity; the introduction of a large load of
20 extra PKA inside the neuron will likely perturb this equilibrium, first by buffering
21 a large part of intracellular cAMP (this in itself may not be a problem) and second
22 by releasing an active PKA subunit that will impact feed-back mechanisms. The
23 PKA-derived probes also suffer from kinetic limitations (see below). Despite all
24 these limitations, the genetically-encoded PKA-based probe has been successfully
25 used on cardiocytes where it reported changes in PKA dissociation state in
26 response to beta-adrenergic stimulation (Mongillo et al., 2004), and it may prove
27 useful in some specific neuronal applications, particularly where a highly
28 sensitive qualitative monitoring is needed. For example, a PKA-based genetically
29 encoded sensor reported responses to activators of the PKA cascade in transgenic
30 *Drosophila*, although probe expression led to severe developmental defects
31 (Lissandron et al., 2007).

32
33
34
35
36
37
38
39
40
41
42
43
44
45
46
47
48
49
50
51
52 Besides PKA, one important target of intracellular cAMP is a family of
53 cyclic-nucleotide gated channels, one of its members being expressed in olfactory
54 neurons. The sensitivity of these membrane channels to cAMP was used to
55 measure changes in sub-membrane cAMP concentration either by
56 electrophysiological recordings or by imaging the calcium influx through these
57 channels (Rich et al., 2001a). This elegant approach showed that the dynamics of
58
59
60
61
62
63
64
65

1
2
3
4 cAMP differ at the membrane and in the cytosol (Rich et al., 2001b).
5 Unfortunately, these channels cannot be expressed in neurons without profoundly
6 affecting their electrophysiological properties. Moreover, as these channels are
7 permeable to calcium, their activation would increase local intracellular calcium
8 level which may affect the cAMP cascade. Further work along this line may
9 eventually lead to reporter channels that may have limited impact on neuronal
10 excitability.
11
12
13
14

15
16 Cyclic AMP directly modulates another important membrane current in
17 neurons, I_h , which is involved in many physiological activities such as the control
18 of the resting membrane potential, rhythmic activity, and integration of synaptic
19 currents (Kaupp and Seifert, 2001). The HCN2 channel contributes to the I_h
20 current, and its intracellular cAMP binding domain was used to create a cytosolic
21 probe, called HCN2-camps. This probe, as most of the probes presented below, is
22 built on the now classical pattern of a domain sensitive to the signal of interest
23 sandwiched between CFP and YFP fluorophores. When cAMP binds to HCN2-
24 camps binding domain, the conformational change that follows decreases FRET
25 between CFP and YFP with an EC_{50} of 6 μ M. This probe proved suitable to
26 monitor changes in cAMP levels in cardiomyocytes (Nikolaev et al., 2006a) and
27 may be very useful in neurons as well.
28
29
30
31
32
33
34
35
36

37
38 Other genetically-encoded fluorescent FRET sensors were derived from
39 another protein family, Epac, a cAMP receptor protein mediating guanine
40 nucleotide exchange activity toward a small guanosine triphosphatase, Rap1. The
41 probe ICUE-1 was constructed from the full-length Epac sequence (DiPilato et al.,
42 2004). ICUE2 (Dunn et al., 2006; Violin et al., 2008) shares its configuration
43
44 **(figure 1A)** with another probe called CFP–Epac(δ DEP-CD)–YFP
45
46 (Ponsioen et al., 2004) that contains Epac1 with a deletion of the N-terminal
47 domain for reducing the attachment to intracellular membrane. Further deletion of
48 Epac keeping only the cAMP-binding domain generated a smaller sensor called
49 Epac1-camps (Nikolaev et al., 2004). Epac has a lower sensitivity to cAMP than
50 PKA, and dose-response curves for this family of probes indicate sensitivities in
51 the micromolar range.
52
53
54
55
56
57
58

59
60 In addition to directly measuring cAMP concentration, the downstream
61 biochemical effect of PKA on protein phosphorylation can also be monitored. A-
62
63
64
65

1
2
3
4 kinase activity reporter (AKAR) is a recombinant protein composed of a
5 phosphoamino acid binding domain and PKA-specific substrate sandwiched
6
7 between CFP and YFP (**figure 1B**). When phosphorylated by PKA,
8
9 intramolecular binding of the substrate by the phosphoamino acid binding domain
10 drives a conformational reorganization, leading to an increase in FRET between
11 CFP and YFP. The FRET response of the first probes in this class, AKAR1
12 (Zhang et al., 2001), was largely irreversible in living cells. It was hypothesized
13 that tight binding of the phosphorylated substrate to the phosphoaminoacid
14 binding domain (which was the 14-3-3 protein) can prevent the phosphorylated
15 substrate from being dephosphorylated by phosphatases and lead to apparent
16 irreversibility of the reporter. In order to continuously monitor the dynamic
17 balance between the kinase and phosphatase activities, however, it is desirable
18 that the kinase activity reporter be reversible. The replacement of the 14-3-3 with
19 FHA1, a modular phosphothreonine binding domain with a weaker binding
20 affinity than that of 14-3-3, led to the generation of AKAR2, a reversible AKAR
21 reporter (Zhang et al., 2005). Additionally, use of GFP variants with a reduced
22 tendency to dimerize (Zacharias et al., 2002) as FRET donor and acceptor in
23 AKAR2.2 helped to improve reversibility (Dunn et al., 2006). In the most recent
24 efforts of sensor optimization, using circular permutants of fluorescent protein to
25 replace wild-type YFP as the FRET acceptor led to improved dynamic range,
26 presumably via changes of the relative orientation of the donor and acceptor
27 fluorophores. AKAR3, the current version of AKAR, utilized a circularly
28 permuted Venus (cpV E172) and doubled the response amplitude of AKAR2
29 (Allen and Zhang, 2006).
30
31
32
33
34
35
36
37
38
39
40
41
42
43
44
45

46 AKAR probes exhibit a FRET increase in response to forskolin (a drug which
47 activates adenylyl-cyclases), and this effect was observed with AKAR2 in cortex,
48 intralaminar thalamic neurons (Gervasi et al., 2007) and ventrobasal thalamus
49 (Gervasi and Vincent, unpublished). AKAR2 also responds to neuromodulators
50 that are positively coupled to the cAMP/PKA cascade, such as serotonin via the 5-
51 HT₇ receptor in thalamic intralaminar neurons (Gervasi et al., 2007). It is
52 important to note that the probe responds to low concentrations of
53 neuromodulators (100 nM 5-CT to activate 5-HT₇ receptors), while neither
54 phosphatases nor phosphodiesterases were blocked. AKAR2 thus has a high
55 sensitivity to report the downstream effect, at the kinase level, of a
56
57
58
59
60
61
62
63
64
65

1
2
3
4 neuromodulatory signal received by a neuron.

5
6 Whether the recorded signal depends on phosphorylation must be verified
7 using a mutant of AKAR2 where the phosphorylated threonine is mutated to an
8 alanine (AKAR2mut). Indeed, several artifacts may affect the fluorescence ratio
9 by differentially affecting the optical properties of the pair of fluorophores. The
10 negative control mutant was tested in several preparations to verify that the
11 measured signal reflected a genuine phosphorylation in the PKA-specific site. As
12 expected, agonists or drugs known to activate PKA in the cortex or in intralaminar
13 thalamic nucleus such as forskolin, dopamine, serotonin, and 5-HT₇ agonists, all
14 failed to induce any fluorescence ratio change with AKAR2mut (Gervasi et al.,
15 2007 and unpublished data).
16
17

18 While the fluorescence change has thus been shown to depend on
19 phosphorylation, the specific involvement of PKA still needs to be evaluated.
20 First, the phosphorylation site of the probe was designed to be specific for PKA.
21 The substrate sequence is based on the specific PKA substrate kemptide (Kemp,
22 1980) and consistent with PKA consensus site of R₋₃-R-x₋₁-S/T-B₊₁, where R is
23 arginine, x refers to any amino acid, B to a hydrophobic residue, and the S or T to
24 the site of phosphorylation (Zetterqvist et al., 1976; Smith et al., 1999). Then,
25 several kinases that have overlapping substrate preferences, such as PKC,
26 CaMKII, PKG, were tested and found to have no major effects on AKAR (Zhang
27 et al., 2001). Finally, it is important to use a specific blocker of PKA to
28 demonstrate that this kinase is indeed responsible for the fluorescence change. In
29 brain slices, PKA was blocked using whole-cell recording with 500 μM R_p-
30 cAMPS in the pipette, which blocked the response mediated by the 5-HT₇
31 receptors (Gervasi et al., 2007).
32
33

34 While the consensus phosphorylation site has been designed to be specific for
35 PKA, several phosphatase types can theoretically dephosphorylate the probe. In
36 the cortex, cantharidin and cyclosporin A which together inhibited protein
37 phosphatases 1, 2A and 2B, were shown to prevent the dephosphorylation of
38 AKAR2 (Gervasi et al., 2007). A more specific pharmacology is now needed to
39 identify the phosphatase(s) involved in this dephosphorylation. Once these
40 phosphatases are identified, the recovery of AKAR2 ratio could be used to
41 monitor phosphatase activities.
42
43
44
45
46
47
48
49
50
51
52
53
54
55
56
57
58
59
60
61
62
63
64
65

Cyclic GMP

Nitric oxide is an unconventional neuromodulator which diffuses across membranes and acts principally by activating cGMP synthesis by the soluble guanylyl cyclase. Various probes have been designed in order to report either the release of NO or the production of cGMP. Despite the considerable importance of NO in neuroscience, few of these probes have been actually used in neurons.

A NO-sensitive probe was designed by fusing the heme-binding domain of guanylyl cyclase with EGFP. This probe, named HBR-GFP, responds to NO by an increase of GFP fluorescence, which can be directly monitored in cells, and a change in the excitation spectrum of the probe, which might be monitored ratiometrically by dual wavelength excitation. EGFP was used as a control to verify that the effects depended on the heme-binding moiety of the protein, and pharmacological blockade of NO synthase confirmed that the recorded signals depended on NO. The onset of the response to NO is in the range of hundred of seconds, making this probe unsuitable to monitor rapid neuronal events. Dissociation of NO from the probe is even slower, so the probe only reports the cumulative release of NO. This probe was used in cerebellum slices to evaluate the radial spread of NO within the cerebellar cortex, showing that NO release as a function of parallel fiber stimulation exhibits an unexpected bell-shaped curve (Namiki et al., 2005).

Downstream of NO, cGMP can be measured directly using PKG as a sensor. These probes named CGY (Sato et al., 2000) and Cygnet-2 (Honda et al., 2001) faithfully report changes in intracellular cGMP concentration (**figure 1C**). Interestingly, although these probes have similar structure and fluorophores, the FRET changes in response to cGMP are in opposite directions. While the selectivity of CGY for cGMP against cAMP is debated (Nikolaev et al., 2006b), Cygnet-2 is clearly insensitive to physiologically-relevant cAMP concentrations and has a Kd for cGMP around 1 μ M (Honda et al., 2005; Nikolaev et al., 2006b). It is important to note that the kinase domain from PKG is inactivated by mutation in the Cygnet-2 probe so as not to phosphorylate proteins that may be involved in this signaling cascade. The CGY sensor has been further modified by fusing it to guanylyl cyclase, thus creating a probe sensitive to low NO concentrations (Sato et al., 2005). This may be useful in neuronal preparations to detect very low NO

1
2
3
4 concentrations. It has been shown, however, that resting NO concentrations are
5 sufficient to elevate intracellular cGMP to a level that can be detected with
6 Cygnet-2 (Hepp et al., 2007).
7
8

9
10 New probes using cGMP-binding domains from PKG or phosphodiesterases
11 have been constructed recently and display faster and/or larger responses. These
12 promising tools have not been tried on neurons yet (Nikolaev et al., 2006b;
13 Russwurm et al., 2007; Nausch et al., 2008).
14
15
16

17 18 **Quantification**

19
20 Probes relying only on a change in fluorescence intensity at one wavelength
21 are inherently more sensitive to various artifactual changes such as instrumental
22 fluctuations, cell movements or changes in probe concentration. FRET probes
23 remedy these problems by producing an opposite change in fluorescence intensity
24 at two different wavelengths, which can be monitored using intensity-based
25 methods. Another detection method called "fluorescence life-time imaging"
26 (FLIM) monitors FRET by the changes in life-time of the donor excited state and
27 this method is also independent on the fluorophore concentration. The various
28 quantification approaches have their specific advantages and drawbacks, as has
29 been described for test CFP-YFP fusion constructs (Domingo et al., 2007). We
30 review here the currently used methods that may be useful for neuronal
31 preparations.
32
33
34
35
36
37
38
39
40
41

42 Ratiometric quantification is the most straightforward method, relying on a
43 single excitation wavelength centered on 436 nm for CFP and dual detection at
44 480 (F480) and 530 nm (F530) for CFP and YFP, respectively, with each image
45 being background corrected. The F530/F480 ratio cancels out artifactual changes
46 in intensity and this ratio is monitored continuously during the experiment as an
47 indicator of FRET changes.
48
49
50
51

52 Ratiometric quantification as well as the other intensity-based quantifications
53 strongly depend on an accurate background subtraction. This background cannot
54 be measured directly, since no reference image can be obtained before the probe is
55 expressed. The background value is usually assumed to be a constant value for the
56 whole image, estimated by measuring the autofluorescence in a region of the
57 preparation where no fluorescent probe is expressed. Errors in background
58
59
60
61
62
63
64
65

1
2
3
4 subtraction can lead to errors in absolute ratio values, and the lesser the
5 fluorescence intensity of the probe, the bigger the error. This may be particularly
6 important when comparing different cells or different cellular domains with
7 different brightness. Indeed, comparisons of small neuronal compartments such as
8 dendritic trees, spines or axon terminals with the much brighter soma require a
9 careful background correction and experimental confirmation with the control
10 inactive probe. When measuring the average ratio over a cellular structure with
11 various intensity levels, dim pixels corresponding to regions of low probe
12 concentration bring a less precise estimate of the ratio value compared to bright
13 pixel where the probe gives a better signal/noise ratio. Dim pixels are usually
14 removed using a fixed (and somewhat arbitrary) threshold. A more objective
15 quantification uses all pixels in the region of interest and calculates an average
16 ratio with each pixel weighted by its intensity (Tsien and Harootunian, 1990).
17
18
19
20
21
22
23
24
25

26 Another error would result from time-dependent changes in background value
27 which would produce a continuous drift of the ratio during the experiment. In
28 practice, all these errors are minimized by recording only cells (or regions of a
29 cell) where the fluorescence intensity is much larger (at least 3 times more) than
30 the autofluorescence. At the other extreme, too high an expression of the probe
31 may lead to probe aggregation or cause a cell to be stressed by too much protein
32 expression, so that a good compromise should be determined and validated by
33 biological controls.
34
35
36
37
38
39
40

41 Quantification errors may also stem from the probe itself. For example,
42 AKAR2 targeted to the nucleus using an NLS signal exhibited a lower average
43 ratio than AKAR2 in the cytosol. This difference was also observed with
44 AKAR2mut, showing that this effect did not reflect a difference in basal PKA
45 activity level but rather indicated that the biophysical environment in the nucleus
46 must be different from the cytosol and differentially affect the CFP-YFP
47 interaction. The molecular basis of this effect remains to be determined.
48
49
50
51
52

53 These factors contribute to some cell-to-cell dispersion in the basal ratio
54 value, which is observed even with the insensitive AKAR2mut probe. As a
55 consequence, an absolute calibration of the ratio cannot be performed unless the
56 minimal ratio value (R_{\min}) and the maximal ratio value (R_{\max}) is measured for
57 each cell in the preparation. Concerning AKAR2, R_{\max} is the ratio when all of the
58
59
60
61
62
63
64
65

1
2
3
4 probe molecules are phosphorylated: this value can be easily measured by adding
5 forskolin at the end of the recording. This drug strongly activates adenylyl
6 cyclases and increases the ratio to a level that is not further increased either by
7 phosphodiesterases (Gervasi et al., 2007) or by phosphatase inhibitors (data not
8 shown), showing that the probe is saturated. This ratio value can thus be
9 considered as equal to R_{max} . But R_{min} is difficult to determine experimentally for
10 AKAR2: phosphatases should be strongly activated while PKA is blocked, a
11 situation difficult to achieve in living cells. Quantification with ratiometric
12 imaging of AKAR2 therefore remains limited to measurements of responses as a
13 percentage of the response to forskolin.
14
15
16
17
18
19
20

21 Quantification could be pushed a bit further with the cGMP-sensitive probe
22 Cygnet-2 thanks to better pharmacological tools (Hepp et al., 2007). Increasing
23 doses of a NO donor produced increasing ratio responses up to a maximal value
24 for 50 μ M DEANO or 100 μ M SNAP. This level was not further increased by
25 blockers of phosphodiesterases, thus representing R_{max} . Guanylyl cyclase could be
26 rapidly and efficiently blocked by 10 μ M ODQ which, together with the strong
27 endogenous phosphodiesterase activity, rapidly led to a ratio level significantly
28 lower than baseline (Hepp et al., 2007). This level can be reasonably assumed to
29 be close to R_{min} .
30
31
32
33
34
35
36

37 When the sensor behaves as a single ligand binding domain, the equations
38 used for ratiometric calcium probes (Grynkiewicz et al., 1985) also apply to
39 cAMP or cGMP:
40
41

$$42 \quad [cXMP] = \beta \cdot K_d \cdot (R - R_{min}) / (R_{max} - R_{min}).$$

43
44
45 In this equation, R_{min} is the ratio measured in the absence of ligand, R_{max} is
46 the ratio when the probe is saturated with the ligand. $\beta \cdot K_d$ (apparent K_d) depends
47 on the imaging setup and can be determined experimentally on cell extracts. This
48 type of quantification has been applied to cultured HEK293 cells expressing
49 ICUE2, assuming that the resting cAMP concentration was well below K_d (*i.e.*
50 resting ratio equals R_{min}), and R_{max} was the ratio in the presence of forskolin
51 (Violin et al., 2008).
52
53
54
55
56
57

58 CFP and YFP are far from perfect fluorophores, and their excitation and emission
59 spectra overlap to some extent. One simple correction involves removing the part
60 of CFP emission "spillover" or "bleed-through" collected at the YFP wavelength
61
62
63
64
65

1
2
3
4 (Dunn et al., 2006; Shafer et al., 2008). However, it is not clear how this
5 correction would improve the signal/noise ratio as it does not provide any
6 additional data from the preparation but merely changes the ratio scale. A more
7 sophisticated method involves the acquisition of a third fluorescence image with
8 excitation of the acceptor and measurement of the acceptor fluorescence (480 nm
9 excitation and 530 nm emission for the CFP/YFP pair). This additional image
10 provides an additional data element directly indicative of the acceptor
11 concentration. These three images are processed through various calculation
12 methods, commonly referred to as "three filter cube method" (Gordon et al., 1998;
13 Hoppe et al., 2002; Zimmermann et al., 2002; Gu et al., 2004), and should provide
14 more accurate estimates of FRET changes. However, these quantifications depend
15 on a careful calibration of the imaging system, and the propagation of errors in the
16 calculation resulting from inaccurate background subtraction or errors in
17 calibration has not been studied carefully.

18
19
20
21
22
23
24
25
26
27
28
29
30
31
32
33
34
35
36
37
38
39
40
41
42
43
44
45
46
47
48
49
50
51
52
53
54
55
56
57
58
59
60
61
62
63
64
65
66
67
68
69
70
71
72
73
74
75
76
77
78
79
80
81
82
83
84
85
86
87
88
89
90
91
92
93
94
95
96
97
98
99
100
101
102
103
104
105
106
107
108
109
110
111
112
113
114
115
116
117
118
119
120
121
122
123
124
125
126
127
128
129
130
131
132
133
134
135
136
137
138
139
140
141
142
143
144
145
146
147
148
149
150
151
152
153
154
155
156
157
158
159
160
161
162
163
164
165
166
167
168
169
170
171
172
173
174
175
176
177
178
179
180
181
182
183
184
185
186
187
188
189
190
191
192
193
194
195
196
197
198
199
200
201
202
203
204
205
206
207
208
209
210
211
212
213
214
215
216
217
218
219
220
221
222
223
224
225
226
227
228
229
230
231
232
233
234
235
236
237
238
239
240
241
242
243
244
245
246
247
248
249
250
251
252
253
254
255
256
257
258
259
260
261
262
263
264
265
266
267
268
269
270
271
272
273
274
275
276
277
278
279
280
281
282
283
284
285
286
287
288
289
290
291
292
293
294
295
296
297
298
299
300
301
302
303
304
305
306
307
308
309
310
311
312
313
314
315
316
317
318
319
320
321
322
323
324
325
326
327
328
329
330
331
332
333
334
335
336
337
338
339
340
341
342
343
344
345
346
347
348
349
350
351
352
353
354
355
356
357
358
359
360
361
362
363
364
365
366
367
368
369
370
371
372
373
374
375
376
377
378
379
380
381
382
383
384
385
386
387
388
389
390
391
392
393
394
395
396
397
398
399
400
401
402
403
404
405
406
407
408
409
410
411
412
413
414
415
416
417
418
419
420
421
422
423
424
425
426
427
428
429
430
431
432
433
434
435
436
437
438
439
440
441
442
443
444
445
446
447
448
449
450
451
452
453
454
455
456
457
458
459
460
461
462
463
464
465
466
467
468
469
470
471
472
473
474
475
476
477
478
479
480
481
482
483
484
485
486
487
488
489
490
491
492
493
494
495
496
497
498
499
500
501
502
503
504
505
506
507
508
509
510
511
512
513
514
515
516
517
518
519
520
521
522
523
524
525
526
527
528
529
530
531
532
533
534
535
536
537
538
539
540
541
542
543
544
545
546
547
548
549
550
551
552
553
554
555
556
557
558
559
560
561
562
563
564
565
566
567
568
569
570
571
572
573
574
575
576
577
578
579
580
581
582
583
584
585
586
587
588
589
590
591
592
593
594
595
596
597
598
599
600
601
602
603
604
605
606
607
608
609
610
611
612
613
614
615
616
617
618
619
620
621
622
623
624
625
626
627
628
629
630
631
632
633
634
635
636
637
638
639
640
641
642
643
644
645
646
647
648
649
650
651
652
653
654
655
656
657
658
659
660
661
662
663
664
665
666
667
668
669
670
671
672
673
674
675
676
677
678
679
680
681
682
683
684
685
686
687
688
689
690
691
692
693
694
695
696
697
698
699
700
701
702
703
704
705
706
707
708
709
710
711
712
713
714
715
716
717
718
719
720
721
722
723
724
725
726
727
728
729
730
731
732
733
734
735
736
737
738
739
740
741
742
743
744
745
746
747
748
749
750
751
752
753
754
755
756
757
758
759
760
761
762
763
764
765
766
767
768
769
770
771
772
773
774
775
776
777
778
779
780
781
782
783
784
785
786
787
788
789
790
791
792
793
794
795
796
797
798
799
800
801
802
803
804
805
806
807
808
809
810
811
812
813
814
815
816
817
818
819
820
821
822
823
824
825
826
827
828
829
830
831
832
833
834
835
836
837
838
839
840
841
842
843
844
845
846
847
848
849
850
851
852
853
854
855
856
857
858
859
860
861
862
863
864
865
866
867
868
869
870
871
872
873
874
875
876
877
878
879
880
881
882
883
884
885
886
887
888
889
890
891
892
893
894
895
896
897
898
899
900
901
902
903
904
905
906
907
908
909
910
911
912
913
914
915
916
917
918
919
920
921
922
923
924
925
926
927
928
929
930
931
932
933
934
935
936
937
938
939
940
941
942
943
944
945
946
947
948
949
950
951
952
953
954
955
956
957
958
959
960
961
962
963
964
965
966
967
968
969
970
971
972
973
974
975
976
977
978
979
980
981
982
983
984
985
986
987
988
989
990
991
992
993
994
995
996
997
998
999
1000

Accepter photobleaching is a classical way to estimate FRET level; however, this destructive method could only be used at the end of a recording, and may thus complement the 3 filter cube method.

Ultimately, absolute FRET quantification would be obtained from the fluorescence lifetime of the FRET donor: the lifetime of the excited state of the donor decreases if the energy is transferred to the acceptor by FRET. This parameter is independent of the probe concentration and is directly related to FRET efficacy. Fluorescence lifetime imaging necessitates a dedicated imaging equipment working with nanosecond resolution. Recordings in the frequency domain are fast enough to report events pertaining to signal integration in neurons, and our preliminary recordings show that this method is indeed promising.

Buffering effects

Whether the expression of a probe perturbs the signal to be measured is an important question. We have tested this in detail with AKAR2 in cortical and thalamic brain slices. First, we verified that the expression of AKAR2 did not overtly affect neuronal properties: whole-cell patch-clamp recording showed that neurons expressing AKAR2 display the expected firing behavior in response to depolarizing or hyperpolarizing current injection (**figure 2**). Then, does a

1
2
3
4 large intracellular concentration of AKAR2, by constituting an extra load of PKA
5 substrate, "buffer" the kinase activity of PKA? This appears unlikely to cause
6 major disturbance, since the kinase turnover rate is relatively fast (Gibbs et al.,
7 1992) and PKA can phosphorylate a large number of endogenous proteins. This
8 was confirmed experimentally in intralaminar thalamic neurons where I_{sAHP} , a
9 PKA-sensitive potassium current, was as efficiently blocked by PKA in neurons
10 expressing AKAR2 as in control neurons, showing that probe expression did not
11 change the efficacy of endogenous PKA (Gervasi et al., 2007).
12
13
14
15
16
17

18 The situation may be different with biosensors that bind cyclic nucleotides,
19 since the sensor is present at several tens of micromolar concentration in the
20 cytosol and may thus strongly buffer any response. A similar buffering problem
21 was encountered when intracellular signaling with the calcium ion was studied in
22 neurons using chemical dyes, but with two main differences: 1) for each open
23 calcium channel, thousands of calcium ions enter the cell per second instead of a
24 few tens of cyclic nucleotide molecules being produced by a cyclase during the
25 same time; 2) calcium ions are heavily buffered by a number of endogenous
26 proteins present in neurons while no buffer seems to exist for cyclic nucleotides.
27 As a consequence, when a chemical calcium dye is present at micromolar
28 concentrations, a level similar or lower to the concentration of endogenous
29 calcium-binding proteins, the calcium influx can be adequately detected optically
30 without too much buffering artifact introduced by the dye. Besides, the diffusible
31 dye actually speeds up the diffusion of calcium inside the cell. In contrast, binding
32 of cyclic nucleotides to a large amount of slower-diffusing biosensor molecules
33 could dampen and/or slow down changes in cyclic nucleotide concentration. If the
34 cells synthesized a small and fixed amount of cyclic nucleotides in response to a
35 stimulation, these molecules would activate a small percentage of the probe and
36 would produce very small ratio changes. These predictions are not confirmed by
37 current data since responses to neuromodulators or to calcium waves can be a
38 large fraction of R_{max} (Nikolaev et al., 2004; Dunn et al., 2006; Shafer et al.,
39 2008), showing that neurons are certainly able to load a large fraction of the probe
40 with cyclic nucleotides. Moreover, the buffering effect of the probe could be
41 tested functionally in *Drosophila*: transgenic flies expressing the Epac1-camps
42 probe in neurons exhibited no major perturbation in their daily locomotor activity,
43 an indicator which is sensitive to changes in the cAMP cascade (Shafer et al.,
44
45
46
47
48
49
50
51
52
53
54
55
56
57
58
59
60
61
62
63
64
65

1
2
3
4 2008). The final cyclic nucleotide concentration must then proceed from a tightly
5 controlled dynamic equilibrium in which cyclases produce a large number of
6 cyclic nucleotide molecules until negative feed-back mechanisms become
7 powerful enough to set a new steady-state level or initiate the recovery.
8
9

10 11 **Dynamic equilibrium of signaling cascades** 12 13 14

15 This is exemplified by thalamic neurons studied in brain slices where a tonic
16 NO production maintains a continuous production of cGMP which could be
17 detected by the Cygnet probe (Hepp et al., 2007). Tonic phosphodiesterase
18 activity keeps the cGMP level constant at an intermediate level; pharmacological
19 tools revealed the strong involvement of type II phosphodiesterase in this cGMP
20 balance (Hepp et al., 2007). From this level, the cGMP concentration can either
21 increase or decrease, depending on the up- or down-regulation of guanylyl cyclase
22 and/or phosphodiesterase. Guanylyl cyclases and phosphodiesterases are thus
23 powerful enzymes whose relative activities set the equilibrium point where the
24 cGMP concentration stabilizes. The buffering effect of Cygnet probably has no
25 effect on this final level but only slows changes from this equilibrium level.
26
27
28
29
30
31
32
33

34 A dynamic equilibrium is also seen in the cAMP/PKA cascade: when
35 phosphodiesterases are blocked with IBMX, the AKAR2 ratio strongly increases
36 (**figure 3**) indicating a tonic adenylyl cyclase activity which is continuously
37 counteracted by phosphodiesterases. In *Drosophila*, cAMP imaging using the
38 Epac1-camps sensor revealed that while most neurons studied in this preparation
39 responded to neuropeptides by a FRET decrease, indicative of an increase in
40 intracellular cAMP concentration, a fraction of the large lateral neurons
41 occasionally responded to the DH31 peptide by a FRET increase, indicative of a
42 decrease in cAMP concentration, *i.e.* a downward modulation of a tonic cAMP
43 level (Shafer et al., 2008).
44
45
46
47
48
49
50
51
52

53 The tonic production of cAMP is sufficient to slightly activate PKA since, in
54 cortical brain slices, the application of phosphatase inhibitors also increases the
55 baseline AKAR2 ratio (Gervasi et al., 2007): the tonic PKA activity is reversed by
56 phosphatases to maintain a steady-state level. Indeed, if AKAR2 was not
57 continuously dephosphorylated, the low basal PKA activity would progressively
58 lead to a maximal phosphorylation of the probe and no further response would be
59
60
61
62
63
64
65

1
2
3
4 observed from this R_{\max} level. Fortunately, experiments show that baseline ratio is
5 well below R_{\max} , and AKAR2 responses to receptor stimulations still remain
6 below this R_{\max} value: maximal stimulation of 5-HT₇ receptors increases the ratio
7 value only to half the response to forskolin (Gervasi et al., 2007) and various
8 neuromodulators in the cortex produce graded ratio responses (**figure 4**).
9
10 AKAR2 should thus be viewed as an indicator of the PKA/phosphatase balance
11 with a sensitivity well suited to report neuromodulatory responses in neurons.
12
13
14
15
16

17 In a review, Houslay and Milligan described some cell types that have low
18 "resting" cascade activity while other cell types display a high turnover of the
19 cascade in a futile cycle (Houslay and Milligan, 1997). This has been later
20 demonstrated using the highly-sensitive cyclic-nucleotide gated channel
21 (C460W/E583M mutation): IBMX has no effect on baseline cAMP concentration
22 on HEK293 cells, while the excitable pituitary-derived cell line GH4C1 shows a
23 large response to IBMX (Rich et al., 2001a). Apparently, the neuronal types so far
24 studied in rodent brain slices and *Drosophila* all belong to the "tonically-active"
25 type for both cAMP and cGMP signaling cascades. Why would neurons benefit
26 from a tonically active signaling cascades? One hypothesis is that a tonically
27 active system allows for much wider range of signal integration than a simple
28 on/off system, as modulation of any of the enzymes in the cascade can produce
29 subtle changes in the steady-state level of the signal. It may also allow for faster
30 responses if both synthesis is increased and degradation is decreased in a
31 coordinated way.
32
33
34
35
36
37
38
39
40
41
42
43

44 **Kinetics of cAMP/PKA events**

45
46
47 The kinetics of a probe largely determine its temporal resolution for
48 monitoring the cellular events. Based on the kinetics of purified PKA enzyme, the
49 PKA-based probes have been suggested to dissociate slowly at low cAMP
50 concentrations (Rich and Karpen, 2002) and would therefore be unsuitable to
51 monitor rapid changes in cAMP concentration. This has been measured with the
52 genetically-encoded cAMP-sensitive probe derived from PKA, which responds to
53 cAMP with a time-course that depends on cAMP concentration: while the probe
54 dissociates within few seconds in response to 2 μ M cAMP, the dissociation takes
55 more than 100 sec at 200 nM concentration (Nikolaev et al., 2004). The PKA-
56
57
58
59
60
61
62
63
64
65

1
2
3
4 based probe FICRhR was nonetheless fast enough to report dynamic events such
5 as signal propagation in dendrites of invertebrate neurons (Bacskai et al., 1993;
6 Hempel et al., 1996) or cAMP transients in *Xenopus* embryonic neurons
7 (Gorbunova and Spitzer, 2002). It should be pointed out that while PKA sensors
8 may report changes at low cAMP concentrations with a notable delay, they
9 nevertheless are true indicators of PKA activation, which in itself is important
10 information.
11

12
13
14
15
16 Direct comparison of different probes was performed in retinal ganglion
17 neurons. It appeared that the signals reported by the PKA-based probe were much
18 slower than those recorded with ICUE2 and AKAR2.2 (Dunn et al., 2006). At
19 first glance, it may be surprising that AKAR2.2 responded more quickly than the
20 PKA-based probe, since PKA is responsible for the FRET change of AKAR2.2.
21 The faster kinetics of AKAR2.2 is likely due to an “amplification” effect as one
22 active PKA molecule is able to phosphorylate multiple AKAR2.2 molecules,
23 producing a signal which is detected before a detectable fraction of PKA is
24 dissociated. Epac1-camps responds in less than a few seconds *in vitro*, which was
25 fast enough to report, in cultured hippocampal neurons, the diffusion of cAMP in
26 the cytosol in response to isoprenaline (Nikolaev et al., 2004). ICUE2 also
27 reported fast signals in rat retinal ganglion neurons (Dunn et al., 2006). These
28 probes are still unique tools in directly reporting dynamic events occurring in the
29 cAMP/PKA cascade at the level of individual neurons.
30

31
32
33
34
35
36
37
38
39
40
41 These kinetic methods should also allow one to further dissect the events
42 occurring within the cascade. In retinal ganglion cells, spontaneous cAMP
43 transients were measured with ICUE-2 with an average onset time-constants of 14
44 s (Dunn et al., 2006). In the same preparation, the PKA-sensitive probe AKAR2.2
45 also reported these fast spontaneous oscillations, although with a slightly slower
46 onset time-constant of 20 s (Dunn et al., 2006). This indicates that the delay
47 between cAMP production and phosphorylation of a PKA substrate is on the order
48 of 6 s, when measured in average over the whole cell. In cardiomyocytes, AKAR2
49 phosphorylation was monitored in response either to flash-photolysis of caged
50 cAMP or stimulation of membrane receptors, showing a $t_{1/2}$ of 5 s and 33 s
51 respectively (Saucerman et al., 2006). Similar values were obtained in
52 intralaminar thalamic neurons, where flash photolysis of caged cAMP increased
53 the AKAR2 ratio within few seconds, faster than the speed of the imaging system
54
55
56
57
58
59
60
61
62
63

1
2
3
4 (Gervasi et al., 2007). On the same neurons, the AKAR2 response to the
5 activation of 5-HT₇ receptors took ~2.5 min to reach 90% of the full signal,
6 demonstrating a fairly long delay between the binding of a neuromodulator to a
7 membrane receptor and the transduction of a signal in the cytosol.
8
9

10 The decay of the cAMP/PKA response can also be studied using these sensors. In
11 cortical neurons, dephosphorylation of AKAR2 took ~1h (Gervasi et al., 2007). In
12 contrast, spontaneous ratio oscillations were detected in retinal ganglion cells
13 using ICUE2 or AKAR2.2, with decreases within ~1 min, indicating that cAMP
14 unbinds from ICUE2 and is degraded by phosphodiesterases while phosphatases
15 dephosphorylate AKAR2.2 almost as rapidly (Dunn et al., 2006). This confirms
16 that the cAMP/PKA cascade is a highly dynamic signaling pathway in retinal
17 ganglion neurons where phosphorylation and dephosphorylation are very active
18 processes. This faster apparent dynamics in retinal ganglion cells than in
19 pyramidal cortical neurons can be related to intrinsic differences in the cascade
20 dynamics between these two neuronal types. The A206K mutations introduced in
21 both fluorophores in AKAR2.2 also helps phosphatases access the
22 phosphorylation site of the probe, although in cardiomyocytes, AKAR2 also
23 seemed to dephosphorylate within few minutes (Saucerman et al., 2006).
24
25
26
27
28
29
30
31
32
33
34

35 **Spatial information**

36
37

38 The subcellular localization of intracellular second messenger signals is
39 particularly important in the case of neuronal cells which exhibit distinct
40 compartments with highly specialized functions. Biochemical approaches have
41 revealed that the enzymes involved in signaling are often organized in functional
42 microdomains, and it is a tantalizing to directly observe intracellular signals at the
43 level of specific cellular compartments or within microcompartments.
44
45
46
47
48

49 Most recordings from neurons using genetically-encoded probes were
50 collected in wide-field imaging with low-noise CCD cameras. Better optical
51 sectioning would be achieved with confocal microscopy using a violet laser as
52 shown in *Drosophila* brains (Shafer et al., 2008). Better penetration would be
53 achieved in mammalian brain slices with two photon confocal imaging. This has
54 been performed with a calcium-sensitive probe using the CFP-YFP FRET pair
55 (Heim et al., 2007). Multiphoton imaging should provide information about
56 cyclic nucleotide signaling in small compartments such as dendritic branches,
57
58
59
60
61
62
63
64
65

1
2
3
4 spines and axon terminals in the complex and dispersive environment of a brain
5 slice. While the optical resolution of current systems can be excellent, one should
6 nevertheless keep in mind that cytosolic probes can diffuse and thus blur a
7 compartmented signal. Indeed, fluorescence recovery after photobleaching
8 (FRAP) experiments with HCN2-camps probe showed a diffusion time-course in
9 the order of seconds within the cytosol (Nikolaev et al., 2006a). It can be expected
10 that other freely-diffusing biosensors with similar sizes, as well as the endogenous
11 targets of the cascade, may also diffuse from the cytosol to local signaling
12 "microdomains". This point could be investigated further by adding to the probes
13 attachment domains to non-diffusible cytosolic structures and comparing the
14 kinetics of the response with those obtained with small diffusible probes.
15
16
17
18
19
20
21
22

23 Other subcellular compartments can also be selectively investigated using the
24 cell's ability to carry the probe into the compartment of interest. The NLS signal
25 sequence was used to target AKAR2 to the nucleus, which appeared strongly
26 labeled while no fluorescence was detected in the cytosol. This nuclear probe
27 showed that phosphorylation events also occurred in the nucleus in response to the
28 activation of receptors at the membrane, but with much slower kinetics than in the
29 cytosol (13 vs 2.5 min) (Gervasi et al., 2007). PKA activation was also monitored
30 at the membrane using a PKA-sensitive potassium current; activation of the same
31 receptors produced a maximal membrane response in 0.5 min. These results show
32 that the membrane, the cytosol and the nucleus of neurons are separate
33 compartments which differentially integrate the same neuromodulatory signal
34 with their own specific time-courses. This observation is consistent with the
35 hypothesis that receptors and enzymes of the cascade are compartmented in
36 signaling microdomains located at the membrane close to target membrane
37 channels, while cAMP/PKA signaling in the cytosol appears more 'diffuse'. To
38 further confirm this model, other targeting sequences should be used to target the
39 AKAR2 probe to such signaling microdomains, using anchoring sequences to
40 AKAPs. While this approach proved very powerful in cell lines (Zhang et al.,
41 2001) it has not been tested in neurons.
42
43
44
45
46
47
48
49
50
51
52
53
54
55

56 Heterogeneous distribution of the probe inside the cell may also affect the
57 recorded signal. This was illustrated with cardiocytes where large molecules of
58 the size of biosensors distribute in a striated pattern, probably as a result of "size
59 exclusion" from the more dense myosin bands (Goaillard et al., 2001). As a result,
60
61
62
63
64
65

1
2
3
4 ratio measurements performed on regions with different fluorescence intensities
5 are differently affected by errors in background subtraction (see above) and
6 comparative measurements may lead to erroneous conclusions.
7

8
9 At the tissue level, imaging methods are also powerful tools for providing
10 simultaneously information from many individual cells, thereby opening the
11 possibility to screen large number of neurons for responses to neuromodulators.
12 This approach was used in *Drosophila*, where the FRET signal from genetically-
13 driven expression of Epac1-camps allowed the authors to compare the effect of
14 various neuropeptides on cAMP levels in identified neurons and to show that a
15 large population of neurons involved in the circadian rhythm of the fly respond to
16 the peptide "pigment dispersing factor" (Shafer et al., 2008). A similar approach is
17 applicable to cortical rat brain slices to screen for positive PKA responses in a
18 large numbers of neurons (**figure 4**). Various neuromodulators were bath-
19 applied and washed-out, while the individual responses of more than 40 neurons
20 were recorded simultaneously with a 10x objective. After the experiment, the slice
21 was examined with a 60x objective to identify pyramidal neurons from their
22 typical morphology (traces shown in red on **figure 4**), and neurons in deep
23 cortical layers. We observed that the deep cortical neurons exhibited a larger
24 response to serotonin than pyramidal neurons (**figure 4**, blue trace and traces
25 below). The slice was then fixed and processed for NeuN immunohistochemistry,
26 which showed that each cell expressing AKAR2 and recorded in this experiment
27 was a neuron. Indeed, other antibodies could be used to reveal key molecular
28 determinants of the neuronal type and thus screen how identified neuronal types
29 respond to series of neuromodulators.
30
31
32
33
34
35
36
37
38
39
40
41
42
43
44
45
46
47
48

49 **Perspectives**

50
51
52 Fast electrical signal transmission in the brain has long been studied using
53 electrophysiological tools, and our knowledge of the functional integration of fast
54 neuronal signals has made considerable progresses during the second half of the
55 last century. The development of bioluminescent and fluorescent calcium
56 indicators has considerably broadened this knowledge by providing spatial
57 information from the subcellular to the network levels. In contrast,
58
59
60
61
62
63
64
65

1
2
3
4 neuromodulatory processes lacked a direct measurement method, as the analysis
5 of these processes mostly relied, on the one hand, on biochemical studies, and on
6 the other hand on pharmacological and genetic methods evaluated *in vivo*. The
7 huge gap between these two levels of analysis is now being filled by a novel
8 experimental approach which uses genetically encoded biosensors to directly
9 monitor specific second messenger responses to neuromodulatory events *ex vivo*
10 and even in the living animal. Indeed, specific expression of a probe in a
11 determined neuron type is now routine genetics in mice, and series of transgenic
12 animals expressing various sensors in diverse brain regions will be created in the
13 next few years. Signaling events will then be recorded directly in brain slices,
14 from the surface of the brain using multiphoton confocal microscopy, or even
15 from deep brain regions using fibered fluorescence microscopy (Vincent et al.,
16 2006). This opens the possibility to reconcile the cellular data obtained from *ex*
17 *vivo* preparations with the integrated data recorded in the physiological context of
18 the living animal. Such an approach will undoubtedly shed new light on the
19 integrative processes carried on in the brain by neuromodulators, and will help
20 elucidate the mechanisms of neuromodulatory integration and its interaction with
21 fast neuronal processing.
22
23
24
25
26
27
28
29
30
31
32
33
34
35

36 Acknowledgements

37
38
39 We would like to thank Pr Ron Harris-Warrick for critically reading this manuscript. This work
40 was supported by CNRS, UPMC, "Fondation pour la Recherche Médicale" and "Fondation pour la
41 Recherche sur le Cerveau" (to P. V.); and by NIH (DK073368 and CA122673), the American
42 Heart Association, the Young Clinical Scientist Award Program of the Flight Attendant Medical
43 Research Institute, and 3M (to J. Z.).
44
45
46
47

48 References:

49
50
51 Adams, S.R. et al. (1991) Fluorescence ratio imaging of cyclic AMP in single
52 cells. *Nature*, **349**, 694-697.
53
54 Allen, M.D. & Zhang, J. (2006) Subcellular dynamics of protein kinase A activity
55 visualized by FRET-based reporters. *Biochemical and Biophysical Research*
56 *Communications*, **348**, 716-721.
57
58
59 Bacskai, B.J. et al. (1993) Spatially resolved dynamics of cAMP and protein
60 kinase A subunits in Aplysia sensory neurons. *Science*, **260**, 222-226.
61
62
63
64
65

1
2
3
4 DiPilato, L.M., Cheng, X. & Zhang, J. (2004) Fluorescent indicators of cAMP and
5 Epac activation reveal differential dynamics of cAMP signaling within discrete
6 subcellular compartments. *Proceedings of the National Academy of Sciences of*
7 *the United States of America*, **101**, 16513-16518.
8
9 Domingo, B. et al. (2007) Imaging FRET standards by steady-state fluorescence
10 and lifetime methods. *Microsc Res Tech*,
11
12 Dunn, T.A. et al. (2006) Imaging of cAMP levels and protein kinase a activity
13 reveals that retinal waves drive oscillations in second-messenger cascades.
14 *Journal of Neuroscience*, **26**, 12807-12815.
15
16 Gervasi, N. et al. (2007) Dynamics of PKA Signaling at the Membrane, in the
17 Cytosol and in the Nucleus of Neurons in Mouse Brain Slices. *Journal of*
18 *Neuroscience*, **27**, 2744-2750.
19
20 Gibbs, C.S. et al. (1992) Systematic mutational analysis of cAMP-dependent
21 protein kinase identifies unregulated catalytic subunits and defines regions
22 important for the recognition of the regulatory subunit. *Journal of Biological*
23 *Chemistry*, **267**, 4806-4814.
24
25 Goaillard, J.-M., Vincent, P. & Fischmeister, R. (2001) Simultaneous
26 measurements of intracellular cAMP and L-type Ca²⁺ current in single frog
27 ventricular myocytes. *Journal of Physiology*, **530**, 79-91.
28
29 Gorbunova, Y.V. & Spitzer, N.C. (2002) Dynamic interactions of cyclic AMP
30 transients and spontaneous Ca(2+) spikes. *Nature*, **418**, 93-96.
31
32 Gordon, G.W. et al. (1998) Quantitative fluorescence resonance energy transfer
33 measurements using fluorescence microscopy. *Biophysical Journal*, **74**, 2702-
34 2713.
35
36 Grynkiewicz, G., Poenie, M. & Tsien, R.Y. (1985) A new generation of Ca²⁺
37 indicators with greatly improved fluorescence properties. *Journal of Biological*
38 *Chemistry*, **260**, 3440-3450.
39
40 Gu, Y. et al. (2004) Quantitative fluorescence resonance energy transfer (FRET)
41 measurement with acceptor photobleaching and spectral unmixing. *Journal of*
42 *Microscopy*, **215**, 162-173.
43
44 Heim, N. et al. (2007) Improved calcium imaging in transgenic mice expressing a
45 troponin C-based biosensor. *Nat Methods*, **4**, 127-129.
46
47 Hempel, C.M. et al. (1996) Spatio-temporal dynamics of cAMP signals in an
48 intact neural circuit. *Nature*, **384**, 166-169.
49
50
51
52
53
54
55
56
57
58
59
60
61
62
63
64
65

1
2
3
4 Hepp, R. et al. (2007) Phosphodiesterase type 2 and the homeostasis of cyclic
5 GMP in living thalamic neurons. *Journal of Neurochemistry*, **102**, 1875-1886.
6
7 Honda, A. et al. (2005) Cygnets: in vivo characterization of novel cGMP
8 indicators and in vivo imaging of intracellular cGMP. *Methods in Molecular*
9 *Biology*, **307**, 27-43.
10
11 Honda, A. et al. (2001) Spatiotemporal dynamics of guanosine 3',5'-cyclic
12 monophosphate revealed by a genetically encoded, fluorescent indicator.
13 *Proceedings of the National Academy of Sciences of the United States of America*,
14 **98**, 2437-2442.
15
16 Hoppe, A., Christensen, K. & Swanson, J.A. (2002) Fluorescence resonance
17 energy transfer-based stoichiometry in living cells. *Biophysical Journal*, **83**, 3652-
18 3664.
19
20 Houslay, M.D. & Milligan, G. (1997) Tailoring cAMP-signalling responses
21 through isoform multiplicity. *Trends in Biochemical Sciences*, **22**, 217-224.
22
23 Kaupp, U.B. & Seifert, R. (2001) Molecular Diversity of Pacemaker Ion
24 Channels. *Annu. Rev. Physiol*, **63**, 235-257.
25
26 Kemp, B.E. (1980) Phosphorylation of acyl and dansyl derivatives of the peptide
27 Leu-Arg-Arg-Ala-Ser-Leu-Gly by the cAMP-dependent protein kinase. *Journal of*
28 *Biological Chemistry*, **255**, 2914-2918.
29
30 Lissandron, V. et al. (2007) Transgenic fruit-flies expressing a FRET-based
31 sensor for in vivo imaging of cAMP dynamics. *Cellular Signalling*, **19**, 2296-
32 2303.
33
34 Lissandron, V. et al. (2005) Improvement of a FRET-based indicator for cAMP
35 by linker design and stabilization of donor-acceptor interaction. *Journal of*
36 *Molecular Biology*, **354**, 546-555.
37
38 Lohse, M.J. et al. (2008) Optical techniques to analyze real-time activation and
39 signaling of G-protein-coupled receptors. *Trends Pharmacol Sci*, **29**, 159-165.
40
41 Mongillo, M. et al. (2004) Fluorescence resonance energy transfer-based analysis
42 of cAMP dynamics in live neonatal rat cardiac myocytes reveals distinct functions
43 of compartmentalized phosphodiesterases. *Circulation Research*, **95**, 67-75.
44
45 Namiki, S. et al. (2005) NO signalling decodes frequency of neuronal activity and
46 generates synapse-specific plasticity in mouse cerebellum. *Journal of Physiology*,
47 **566**, 849-863.
48
49
50
51
52
53
54
55
56
57
58
59
60
61
62
63
64
65

1
2
3
4 Nausch, L.W. et al. (2008) Differential patterning of cGMP in vascular smooth
5 muscle cells revealed by single GFP-linked biosensors. *Proceedings of the*
6 *National Academy of Sciences of the United States of America*, **105**, 365-370.

7
8
9 Nikolaev, V.O. et al. (2004) Novel single chain cAMP sensors for receptor-
10 induced signal propagation. *Journal of Biological Chemistry*, **279**, 37215-
11
12
13
14 **37218**.

15
16 Nikolaev, V.O. et al. (2006a) Cyclic AMP Imaging in Adult Cardiac Myocytes
17 Reveals Far-Reaching β 1-Adrenergic but Locally Confined β 2-
18 Adrenergic Receptor-Mediated Signaling. *Circulation Research*, **99**, 1084-1091.

19
20 Nikolaev, V.O., Gambaryan, S. & Lohse, M.J. (2006b) Fluorescent sensors for
21 rapid monitoring of intracellular cGMP. *Nature Methods*, **3**, 23-25.

22
23 Ponsioen, B. et al. (2004) Detecting cAMP-induced Epac activation by
24 fluorescence resonance energy transfer: Epac as a novel cAMP indicator. *EMBO*
25 *Reports*, **5**, 1176-1180.

26
27 Rich, T.C. & Karpen, J.W. (2002) Review article: cyclic AMP sensors in living
28 cells: what signals can they actually measure? *Ann Biomed Eng*, **30**, 1088-1099.

29
30 Rich, T.C. et al. (2001a) In vivo assessment of local phosphodiesterase activity
31 using tailored cyclic nucleotide-gated channels as cAMP sensors. *Journal of*
32 *General Physiology*, **118**, 63-78.

33
34 Rich, T.C. et al. (2001b) A uniform extracellular stimulus triggers distinct cAMP
35 signals in different compartments of a simple cell. *Proceedings of the National*
36 *Academy of Sciences of the United States of America*, **98**, 13049-13054.

37
38 Russwurm, M. et al. (2007) Design of fluorescence resonance energy transfer
39 (FRET)-based cGMP indicators: a systematic approach. *Biochemical Journal*,
40
41 **407**, 69-77.

42
43 Sato, M., Hida, N. & Umezawa, Y. (2005) Imaging the nanomolar range of nitric
44 oxide with an amplifier-coupled fluorescent indicator in living cells. *Proceedings*
45 *of the National Academy of Sciences of the United States of America*,

46
47 Sato, M. et al. (2000) Fluorescent indicators for cyclic GMP based on cyclic
48 GMP-dependent protein kinase I α and green fluorescent proteins. *Analytical*
49 *Chemistry*, **72**, 5918-5924.

1
2
3
4 Saucerman, J.J. et al. (2006) Systems analysis of PKA-mediated phosphorylation
5 gradients in live cardiac myocytes. *Proceedings of the National Academy of*
6 *Sciences of the United States of America*, **19**, 2650-2658.
7
8 Shafer, O.T. et al. (2008) Widespread Receptivity to Neuropeptide PDF
9 throughout the Neuronal Circadian Clock Network of Drosophila Revealed by
10 Real-Time Cyclic AMP Imaging. *Neuron*, **58**, 161-163.
11
12 Smith, C.M. et al. (1999) The catalytic subunit of cAMP-dependent protein
13 kinase: prototype for an extended network of communication. *Prog Biophys Mol*
14 *Biol*, **71**, 313-341.
15
16 Tsien, R.Y. & Harootunian, A.T. (1990) Practical design criteria for a dynamic
17 ratio imaging system. *Cell Calcium*, **11**, 93-109.
18
19 Vincent, P. et al. (2006) Live imaging of neural structure and function by fibred
20 fluorescence microscopy. *EMBO Reports*, **7**, 1154-1161.
21
22 Vincent, P. & Bruscianno, D. (2001) Cyclic AMP imaging in neurones in brain
23 slice preparations. *Journal of Neuroscience Methods*, **108**, 189-198.
24
25 Violin, J.D. et al. (2008) β 2-Adrenergic Receptor Signaling and Desensitization
26 Elucidated by Quantitative Modeling of Real Time cAMP Dynamics. *Journal of*
27 *Biological Chemistry*, **283**, 2949-2961.
28
29 Willoughby, D. & Cooper, D.M. (2008) Live-cell imaging of cAMP dynamics.
30 *Nature Methods*, **5**, 29-36.
31
32 Zacco, M. et al. (2000) A genetically encoded, fluorescent indicator for cyclic
33 AMP in living cells. *Nature Cell Biology*, **2**, 25-29.
34
35 Zacharias, D.A. et al. (2002) Partitioning of lipid-modified monomeric GFPs into
36 membrane microdomains of live cells. *Science*, **296**, 913-916.
37
38 Zetterqvist, O. et al. (1976) The minimum substrate of cyclic AMP-stimulated
39 protein kinase, as studied by synthetic peptides representing the phosphorylatable
40 site of pyruvate kinase (type L) of rat liver. *Biochemical and Biophysical*
41 *Research Communications*, **70**, 696-703.
42
43 Zhang, J. et al. (2005) Insulin disrupts beta-adrenergic signalling to protein kinase
44 A in adipocytes. *Nature*, **437**, 569-573.
45
46 Zhang, J. et al. (2001) Genetically encoded reporters of protein kinase A activity
47 reveal impact of substrate tethering. *Proceedings of the National Academy of*
48 *Sciences of the United States of America*, **98**, 14997-15002.
49
50
51
52
53
54
55
56
57
58
59
60
61
62
63
64
65

1
2
3
4 Zimmermann, T. et al. (2002) Spectral imaging and linear un-mixing enables
5 improved FRET efficiency with a novel GFP2-YFP FRET pair. *FEBS Letters*,
6 **531**, 245-249.
7
8
9

10 **Figure legends**

11
12
13 Table 1: biosensors for cyclic nucleotides.

14
15 Figure 1: schematic representation of probes for cyclic nucleotide signaling. A: ICUE2 (and other
16 Epac-derived cAMP-sensitive probes) contains one cAMP-binding site from Epac. Binding of one
17 cAMP molecule induces a conformational change that decreases FRET. B: AKAR2 contains a
18 PKA consensus phosphorylation site and a FHA domain. When the threonine is phosphorylated by
19 PKA, the FHA domain binds to it, increasing FRET. For all probes, the conformational change is
20 reversible upon cyclic nucleotide unbinding or phosphatase-mediated dephosphorylation. C:
21 Cygnet2 is constituted of the regulatory and catalytic domains of PKG with CFP and YFP fused at
22 N- and C-terminals respectively. Binding of two cGMP to the regulatory subunit induce a
23 conformational change which results in a FRET decrease.
24
25
26
27

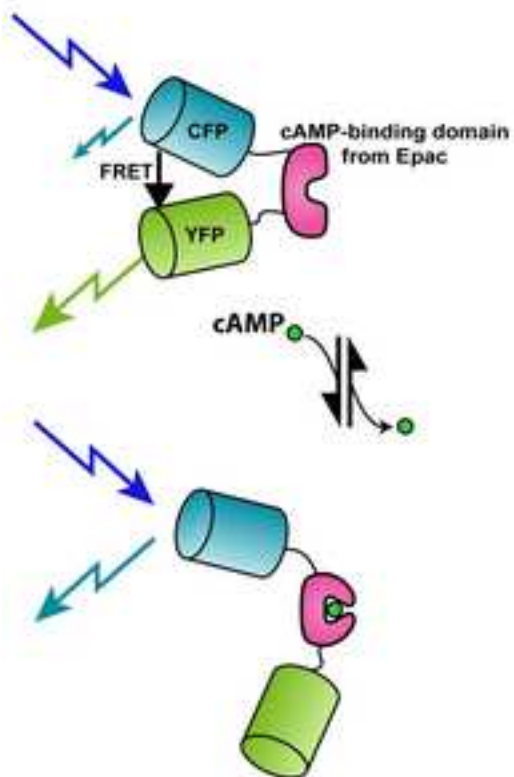
28
29 Figure 2: Expression of the probe does not affect the firing properties of neurons in brain slices.
30 Left: image combining transillumination and epifluorescence. Right: current-clamp recording of
31 the same neuron upon depolarizing and hyperpolarizing current injection. A: a thalamocortical
32 neuron in the ventrobasal complex displays the characteristic tonic firing upon depolarization.
33 Hyperpolarization induces the 'sag', followed by low-threshold calcium spike upon repolarization.
34 B: a layer V pyramidal cortical neuron fires tonically upon depolarization.
35
36
37

38
39 Figure 3: Blocking phosphodiesterases increases PKA activity. A thalamocortical neuron in the
40 ventrobasal complex in a thalamic brain slice is recorded with the AKAR2 probe. IBMX strongly
41 increases the F535/F480 fluorescence ratio, indicating a strong activation of PKA that is not
42 further increased by subsequent forskolin application. Top: YFP fluorescence image (left) and
43 pseudocolor images in control (middle) and during bath application of IBMX (right). Calibration
44 squares indicate the intensity range (from left to right) in counts/pixel/s and the ratio range (from
45 bottom to top). The size of the square is 10 μ m. The graph shows the average ratio measured over
46 the cell during the experiment.
47
48
49

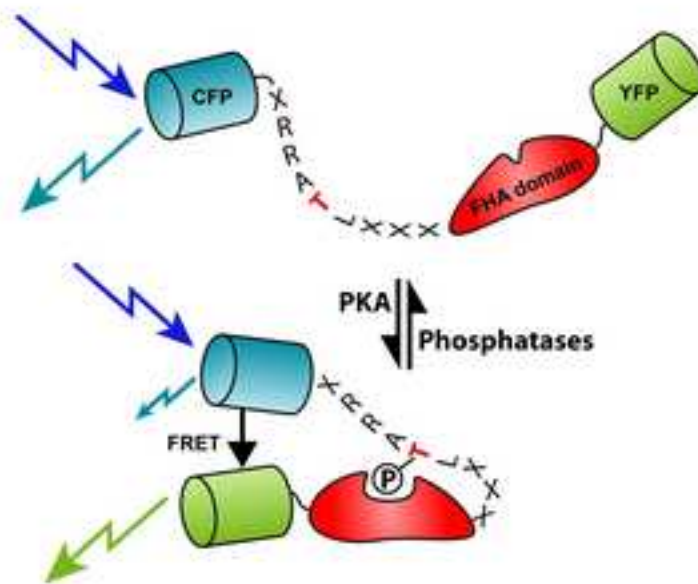
50
51 Figure 4: Cortical brain slice expressing AKAR2 and recorded with a 10x objective. A:
52 Pseudocolor images in control (top) and during dopamine application (bottom). B: 40 neurons
53 were analyzed for their F535/F480 ratio change during bath application of noradrenaline,
54 dopamine, 5-HT and forskolin. After the recording, at least 9 cells (red traces) were
55 unambiguously identified as pyramidal neurons from their morphology. Other cells (blue trace and
56 below) were in layer VI and were not pyramidal neurons. C: the slice was fixed and the same
57 neurons were examined with a 60x objective for AKAR fluorescence (top image) and NeuN
58 immunoreactivity (bottom image).
59
60
61
62
63
64
65

Figure1
[Click here to download high resolution image](#)

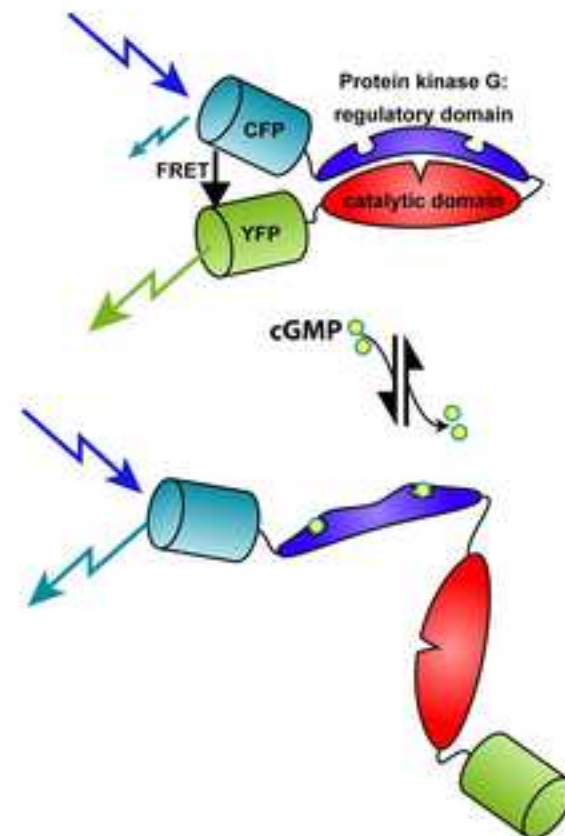
A: ICUE2



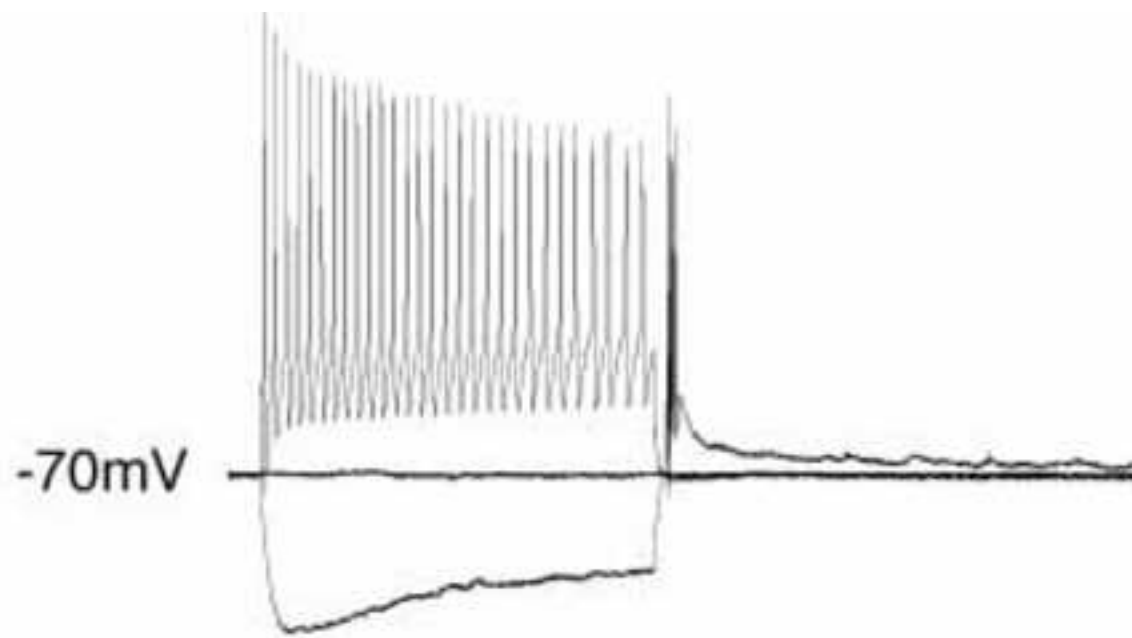
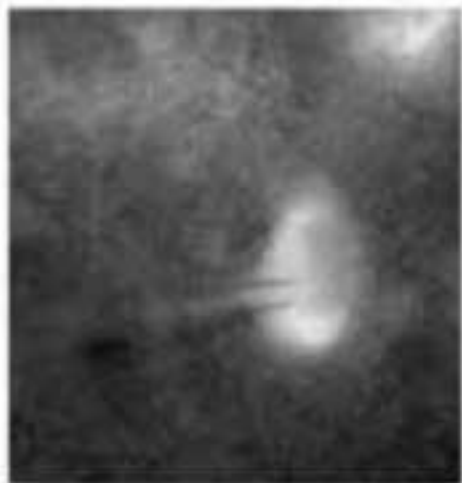
B: AKAR2



C: Cygnet 2



A



B

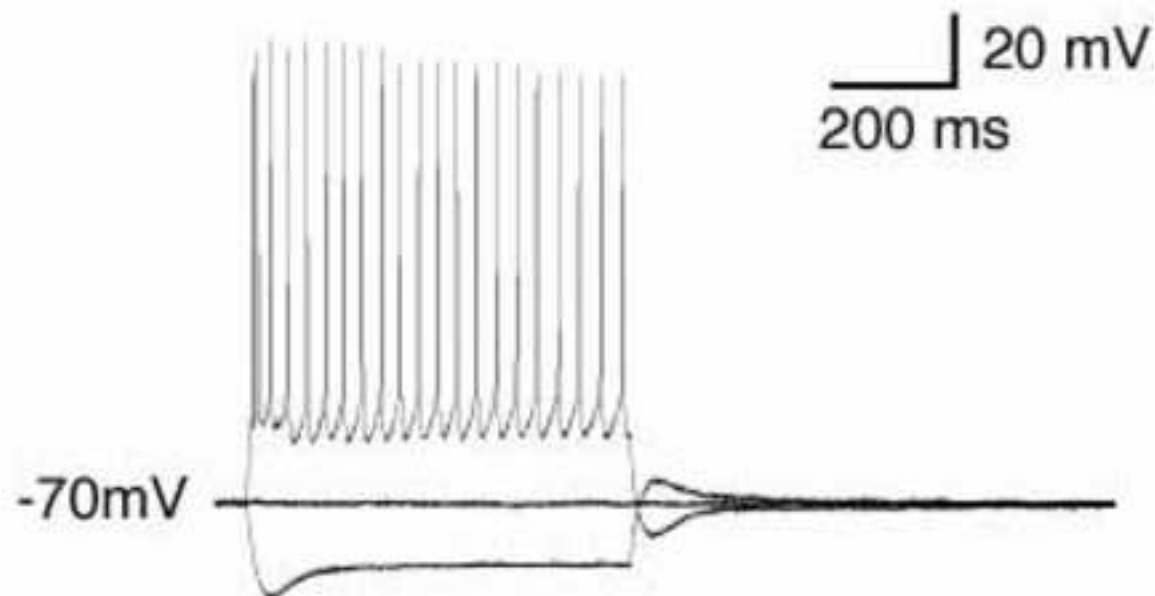
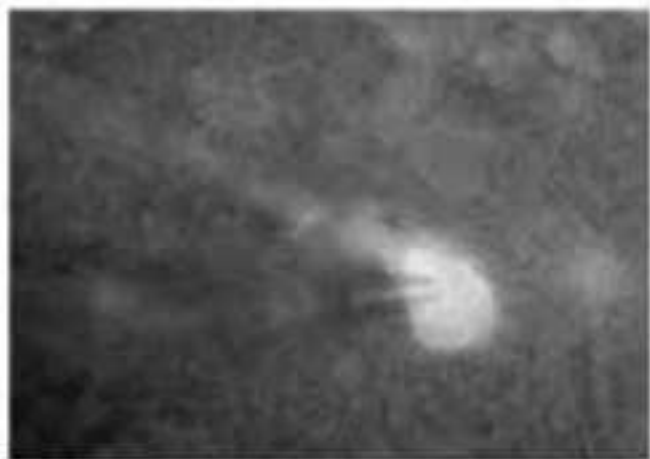


Figure3

[Click here to download high resolution image](#)

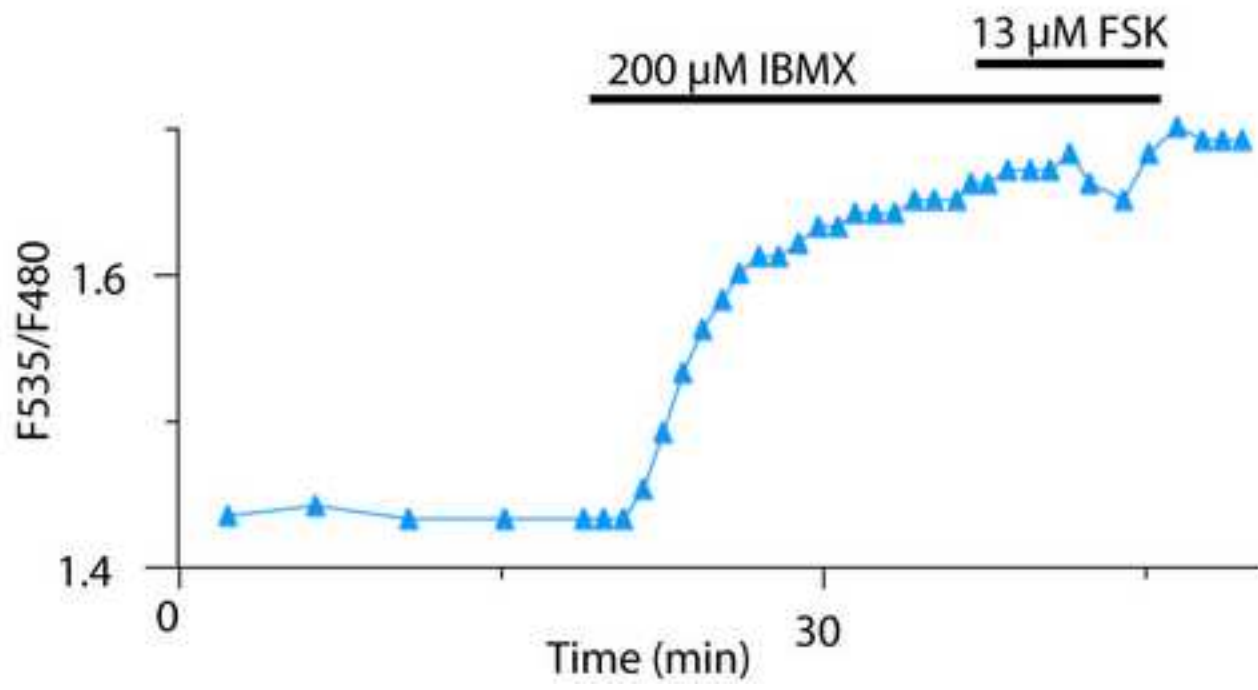
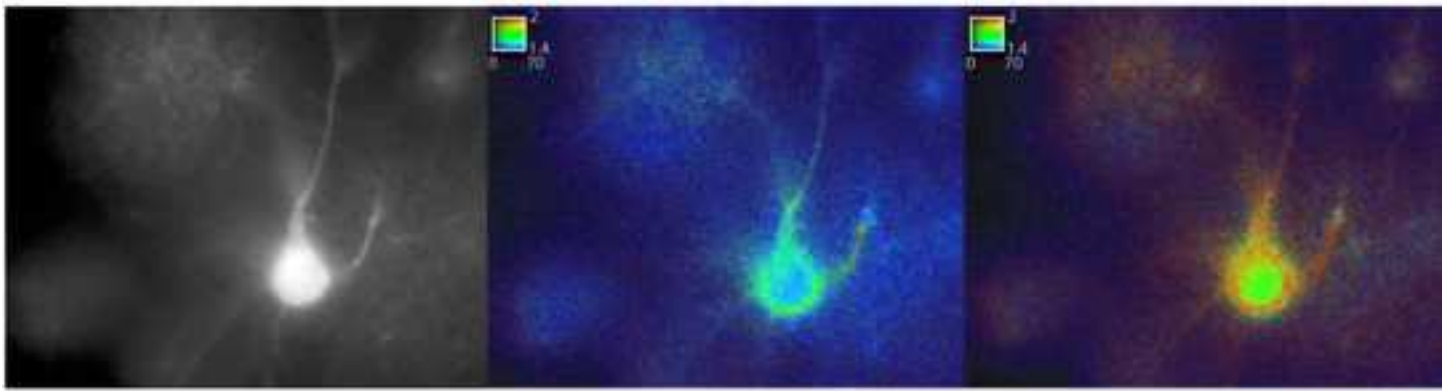
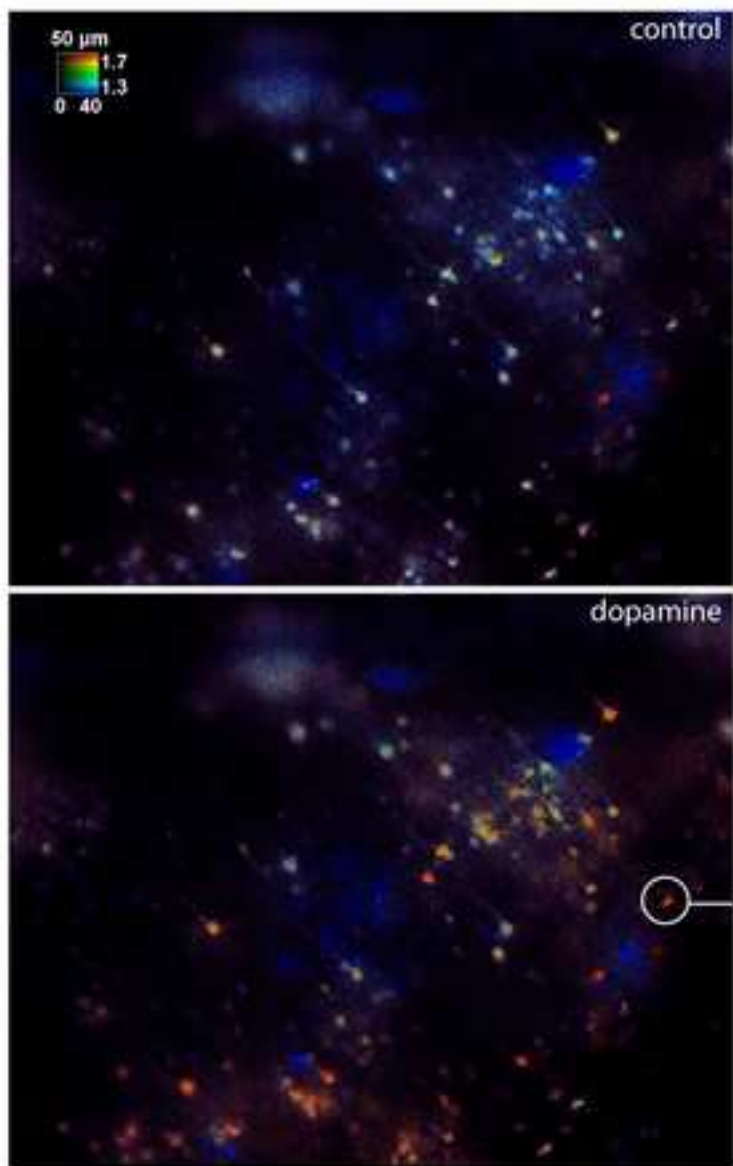
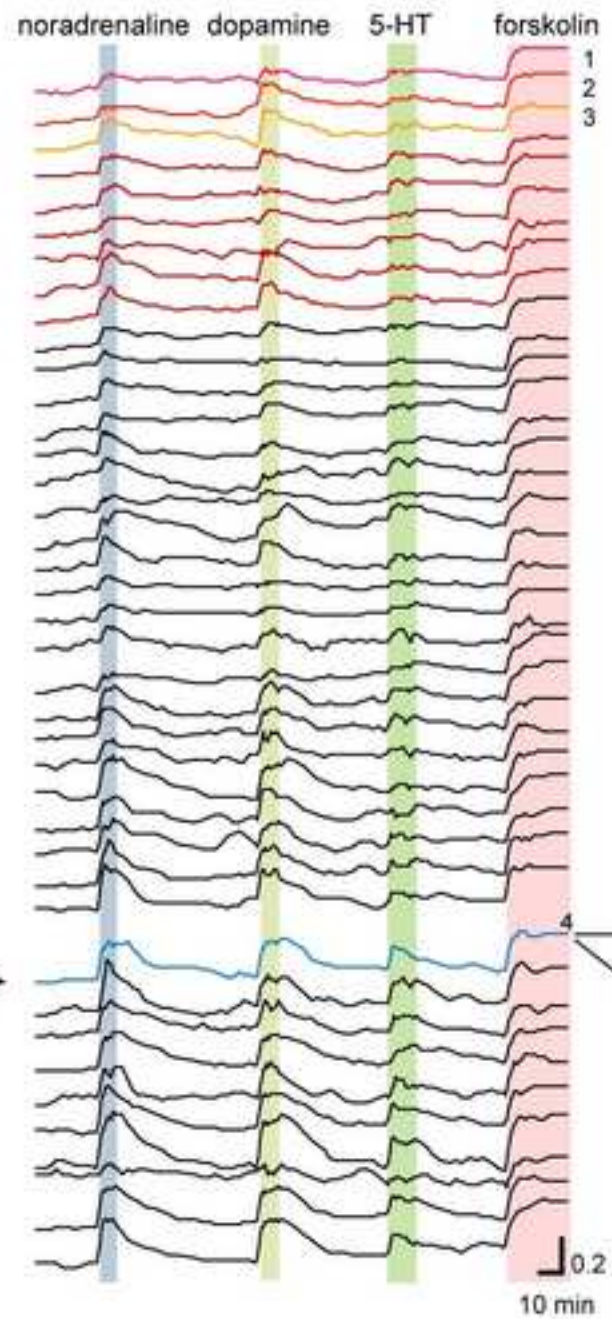


Figure4
[Click here to download high resolution image](#)

A



B



C

